

# Higher-Order Band Topology and Corner Charges in Monolayer Graphdiyne

Eunwoo Lee,<sup>1,2,3,\*</sup> Rokyeon Kim,<sup>1,2,\*</sup> Junyeong Ahn,<sup>1,2,3</sup> and Bohm-Jung Yang<sup>1,2,3,†</sup>

<sup>1</sup>*Department of Physics and Astronomy, Seoul National University, Seoul 08826, Korea*

<sup>2</sup>*Center for Correlated Electron Systems, Institute for Basic Science (IBS), Seoul 08826, Korea*

<sup>3</sup>*Center for Theoretical Physics (CTP), Seoul National University, Seoul 08826, Korea*

(Dated: December 15, 2024)

Based on first-principles calculations and tight-binding model analysis, we propose monolayer graphdiyne as a candidate material for a two-dimensional higher-order topological insulator protected by the combination of time-reversal  $T$  and inversion  $P$  symmetries. Due to the nontrivial higher-order band topology characterized by a two-dimensional topological invariant  $w_2$ , so-called the second Stiefel-Whitney number, monolayer graphdiyne hosts localized states at mirror invariant corners. Although its low-energy band structure can be properly described by using only the  $p_z$  orbital of each carbon atom, the corresponding bulk band topology is trivial with  $w_2 = 0$ . The nontrivial higher-order band topology with  $w_2 = 1$  can be correctly captured only when the contribution from the core electronic levels derived from  $s$ ,  $p_x$ ,  $p_y$  orbitals are included, which is further confirmed by the Wilson loop and the nested Wilson loop calculations. We show that the higher-order band topology of a monolayer graphdiyne is the fundamental origin of the nontrivial band topology of the corresponding three-dimensional material, ABC-stacked graphdiyne, which hosts monopole nodal lines in the bulk and hinge states along the sample boundary.

PACS numbers:

*Introduction.*— Bulk-boundary correspondence is a fundamental property of topological phases. In conventional topological insulators, the gapped bulk states in  $d$ -dimensions support metallic states in  $(d-1)$ -dimensional surfaces. Recently, however, a class of topological crystalline insulators violating the conventional bulk-boundary correspondence are proposed, and they are nowadays called higher-order topological insulators (HOTIs). In contrast to the conventional topological insulators, the gapless excitations of a HOTI in  $d$ -dimensions are localized in a subspace with a dimension lower than  $(d-1)$ , such as corners or hinges, when the global shape of the material satisfies the crystalline symmetry relevant to the nontrivial bulk band topology [1–5, 7–12]. Recently, rhombohedral bismuth is identified as the first example of three-dimensional (3D) HOTIs hosting helical hinge states [4]. Also there are other theoretical proposals for candidate materials of 3D HOTIs including transition metal dichalcogenides  $\text{MoTe}_2$ ,  $\text{WTe}_2$  hosting helical hinge states [12] and  $\text{Bi}_{2-x}\text{Sm}_x\text{Se}_3$  having chiral hinge states [9].

Two-dimensional (2D) systems can also exhibit a higher-order band topology that hosts gapless states localized at the corners [2, 7, 8, 13, 14]. Contrary to 3D HOTIs, however, there are not many theoretical proposals for candidate materials realizing 2D HOTIs. For instance, phosphorene is one system proposed as a candidate for 2D HOTIs based on a simple tight-binding model calculation [15]. However, in this system, the corner states are protected not by a 2D topological invariant but by a 1D topological invariant, i.e., the charge polarization [15]. Another candidate is twisted bilayer graphene, which can also exhibit higher-order band topology at small twist angles. However, to realize the corner states in this system, the twist angle as well as the chemical potential should be properly controlled [13].

In this Letter, we theoretically propose a monolayer graphdiyne (MGD) as the first realistic candidate material for

a 2D higher-order topological insulator (HOTI) hosting corner charges. Based on first-principles calculations and tight-binding model analysis, we show that a MGD is a HOTI characterized by a 2D topological invariant  $w_2$ , so-called the second Stiefel-Whitney number that is quantized when the system is invariant under the combined operation of time-reversal  $T$  and inversion  $P$  symmetries [16]. To confirm the bulk band topology, we have computed both the Wilson loop and nested Wilson loop spectra, which consistently give a nontrivial 2D invariant  $w_2 = 1$ . Due to the nontrivial  $w_2$ , a finite-size system preserving a mirror symmetry  $M_y : y \rightarrow -y$  can host fractional charges localized at  $M_y$  invariant corners. Interestingly, we find that, although the low-energy band structure can be well-described by using only the states derived from the  $p_z$  orbitals of each carbon atom, the relevant band topology of such a simplified model is trivial with  $w_2 = 0$ . To describe the nontrivial band topology, it is essential to include the contribution from the core electronic levels derived from  $p_{x,y}$  and  $s$  orbitals. Finally, we show that the vertical stacking of graphdiyne layers, which is realized in ABC-stacked graphdiyne [17], generates a 3D nodal line semimetal with  $Z_2$  monopole charge [16], which exhibits hinge states for the range of vertical momentum  $k_z$  between two nodal lines. The fundamental origin of such hinge modes of a nodal line semimetal is the higher-order band topology associated with the nonzero  $w_2$  [9].

*Monolayer graphdiyne.*— Fig. 1(a) describes the unit cell of MGD composed of 18 carbon atoms. Since spin-orbit coupling (SOC) is negligible, MGD can be regarded as a spinless fermion system. The lattice has  $P$ ,  $T$ , a two-fold rotation about the  $x$ -axis  $C_{2x}$ , a six-fold rotation about the  $z$ -axis  $C_{6z}$ , and a mirror  $M_z : z \rightarrow -z$  symmetries. Also, due to the bipartite structure of the lattice, MGD has chiral (or sublattice) symmetry when only the nearest neighbor hopping between different sublattices is considered, similar to the case of

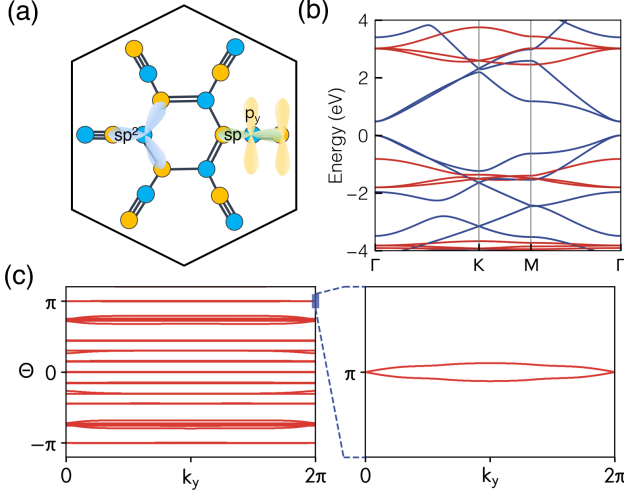


FIG. 1: (Color online) (a) A schematic figure describing the unit cell and the relevant atomic orbitals of a monolayer graphdiyne (MGD) composed of 18 carbon atoms. Two sublattices are marked with yellow and blue colors, respectively. Since MGD has a bipartite lattice structure, chiral symmetry exists when only the nearest neighbor hoppings are considered. (b) The band structure of MGD obtained by first-principles calculations, which shows approximate chiral symmetry near the Fermi level. Since  $p_z$  orbitals are odd while  $s$ ,  $p_x$ ,  $p_y$  orbitals are even under the mirror  $M_z : z \rightarrow -z$  operation, the energy spectrum from  $p_z$  orbitals (blue) is not hybridized with that from  $s$ ,  $p_x$ ,  $p_y$  orbitals (red). (c) The Wilson loop spectrum computed including  $s$ ,  $p_x$ ,  $p_y$ ,  $p_z$  orbitals. The spectrum exhibits a crossing point at  $\theta = \pi$ ,  $k_y = 0$ , which indicates the nonzero second Stiefel-Whitney number  $w_2 = 1$ .

graphene.

Fig. 1(b) shows the band structure along high symmetry directions obtained by first-principles calculations. Here the blue color indicates the bands derived from  $p_z$  orbitals while the red color denotes the bands derived from  $s$ ,  $p_x$ ,  $p_y$  orbitals. Since  $p_z$  orbitals are odd whereas  $s$ ,  $p_x$ ,  $p_y$  orbitals are even under the  $M_z$  operation, the energy spectrum from  $p_z$  orbitals is not hybridized with that from  $s$ ,  $p_x$ ,  $p_y$  orbitals. One can see that the low-energy band structure has approximate chiral symmetry and can be effectively described by using only  $p_z$  orbitals. However, to capture the higher-order band topology, the core electronic states derived from  $s$ ,  $p_x$ ,  $p_y$  orbitals should be included. Namely, although the core electronic states are not important to describe the low-energy band structure, they play a critical role to characterize the bulk band topology as shown below.

In general, a 2D  $PT$ -symmetric spinless fermion system carries three  $\mathbb{Z}_2$  topological invariants,  $w_{1x}$ ,  $w_{1y}$ , and  $w_2$ . Here  $w_{1x}$  ( $w_{1y}$ ) indicates the first Stiefel-Whitney number computed along the  $k_x$  ( $k_y$ ) direction, and  $w_2$  is the second Stiefel-Whitney number. In terms of the sewing matrix  $G_{mn}(\mathbf{k}) = \langle u_{m\mathbf{k}} | PT | u_{n\mathbf{k}} \rangle$ ,  $w_{1a}$  ( $a = x, y$ ) is given by its

one-dimensional (1D) winding number as

$$w_{1a} = -\frac{i}{2} \oint_C \nabla_{\mathbf{k}_a} \log \det G(\mathbf{k}) \pmod{2}, \quad (1)$$

which is equivalent to the quantized Berry phase  $\Phi_a$ , that is,  $\Phi_a = \pi w_{1a} \pmod{2\pi}$ . When the system is  $P$ -symmetric,  $w_{1a}$  is determined by the relation  $(-1)^{w_{1a}} = \prod_{i=1}^2 \xi(\Gamma_{ia})$  where  $\xi(\Gamma_{ia})$  ( $i = 1, 2$ ) is the product of parity eigenvalues of occupied states at the time-reversal invariant momentum (TRIM)  $\Gamma_{ia}$ , and  $\Gamma_{1a}$ ,  $\Gamma_{2a}$  are two TRIMs along the reciprocal lattice vector  $G_a$ . Since  $w_{1a}$  is equivalent to the quantized charge polarization along the  $G_a$  direction, it can be considered as a 1D topological invariant.

On the other hand,  $w_2$  is a 2D topological invariant given by the 2D winding number of the sewing matrix  $G(\mathbf{k})$  modulo 2 [11], and measures the higher-order band topology of  $PT$ -symmetric spinless fermion systems [13, 16]. When the system is  $P$ -symmetric,  $w_2$  can be determined by using the parity eigenvalues of occupied bands at TRIMs [16] as

$$(-1)^{w_2} = \prod_{i=1}^4 (-1)^{[N_{\text{occ}}^-(\Gamma_i)/2]}, \quad (2)$$

where  $N_{\text{occ}}^-(\Gamma_i)$  is the number of occupied bands with an odd parity at the TRIM  $\Gamma_i$ . This expression is equivalent to the  $\mathbb{Z}_4$  classification of  $P$ -symmetric systems, which indicates double band inversion with respect to trivial insulators [20–25].

Using the band structure from first-principles calculations and the corresponding parity eigenvalues at TRIMs, one can easily show that MGD is a higher-order topological insulator with  $w_{1x} = w_{1y} = 0$  and  $w_2 = 1$ . One interesting feature of the MGD band structure is that we get  $w_2 = 0$  when only the bands derived from  $p_z$  orbitals are considered. Namely, although the low-energy band structure itself can be well-described by using only the bands derived from  $p_z$  orbitals, the band topology can be correctly described only when the core electronic states derived from  $s$ ,  $p_x$ ,  $p_y$  orbitals are included. This result can be confirmed by tight-binding analysis as well as the first-principles calculations. Since the bands derived from  $p_z$  orbitals do not hybridize with those derived from other orbitals because of  $M_z$  symmetry, one can compute the relevant topological invariants separately.

The orbital dependence of  $w_2$  can also be confirmed by computing  $w_2$  using the Wilson loop method [13, 16, 26, 27]. The Wilson loop is a gauge-invariant quantity that is defined as a path ordered product of the exponential of Berry connections [28, 29],

$$W_{(k_1+2\pi, k_2) \leftarrow (k_1, k_2)} = \lim_{N \rightarrow \infty} F_{N-1} F_{N-2} \cdots F_1 F_0, \quad (3)$$

where  $[F_i]_{mn} = \langle u_m(\frac{2\pi(i+1)}{N}, k_2) | u_n(\frac{2\pi i}{N}, k_2) \rangle$ . Computed along the  $k_1$  direction parallel to the reciprocal lattice vector  $\mathbf{G}_1$  from  $(k_1, k_2)$ , the set of Wilson loop eigenvalues  $\{e^{i\nu_i(k_2)}\}$  indicates the position of Wannier centers at given  $k_2$ , and the corresponding total charge polarization is given

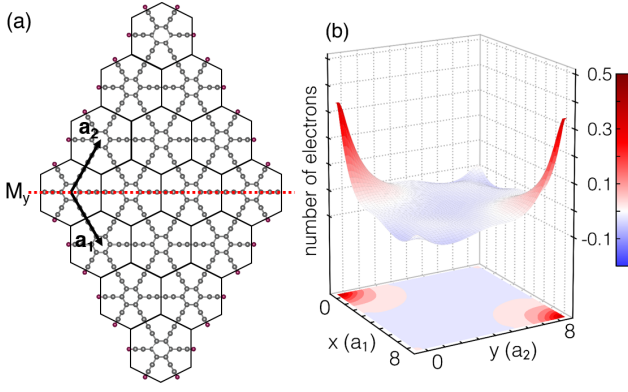


FIG. 2: (Color online) (a) A finite-size structure of MGD preserving  $PT$  symmetry designed to observe the higher-order band topology protected by  $PT$  symmetry. (b) Electron density distribution for a finite-size MGD composed of  $9 \times 9$  unit cells where hydrogen atoms are attached at every corner except at the two  $M_y$  invariant corners. Corner charges related by inversion symmetry appear due to  $w_2 = 1$ .

by  $p_1(k_2) = \frac{1}{2\pi} \sum_i \nu_i(k_2)$ . The Wilson loop spectrum of MGD shows that the charge polarization is zero in both  $k_1$  and  $k_2$  directions, which is consistent with the parity eigenvalue analysis. Also, the single linear-crossing at  $(k_y, \nu) = (0, \pi)$  indicates  $w_2 = 1$  [16]. The nontrivial  $w_2$  can be further confirmed by computing the nested Wilson loop that measures the higher-order band topology [5, 9]. In the presence of  $PT$  symmetry, the Wilson loop spectrum can be divided into two sub-bands that are separated by a gap, each centered at  $\nu = 0$  or  $\nu = \pi$ , respectively. When the Wilson loop operator at given  $k_2$  is diagonalized as

$$W_{(k_1+2\pi, k_2) \leftarrow (k_1, k_2)} = \sum_i |\nu_i(k_2)\rangle e^{i\nu_i(k_2)} \langle \nu_i(k_2) |, \quad (4)$$

using the set of eigenvectors corresponding to the sub-band centered at  $\nu = \pi$ , the nested Wilson loop operator  $\tilde{W}$  along the  $\mathbf{G}_2$  vector is defined as

$$\tilde{W}_{(k_2+2\pi) \leftarrow (k_2)} = \lim_{N \rightarrow \infty} \tilde{F}_{N-1} \tilde{F}_{N-2} \cdots \tilde{F}_0, \quad (5)$$

where  $[\tilde{F}_i]_{mn} = \langle \nu_m(\frac{2\pi(i+1)}{N}) | \nu_n(\frac{2\pi i}{N}) \rangle$ . Since the determinant of the nested Wilson loop operator  $\det(\tilde{W})$  is identical to  $(-1)^{w_2}$  [13], we find that  $\det(\tilde{W})$  is nontrivial. Projecting the Wilson loop operator into the  $p_z$  orbital basis, we observe that the corresponding nested Wilson loop spectrum is trivial. On the other hand, within the  $s$ ,  $p_x$ , and  $p_y$  orbital basis, the nested Wilson loop spectrum is nontrivial, which confirms that the higher-order band topology originates from the core electronic levels [6].

*Corner charges.*— The higher-order band topology of MGD with  $w_2 = 1$  induces a pair of anomalous corner states. To confirm this, let us consider a finite-size structure invariant under  $PT$  symmetry. A tight-binding model analysis shows that when the system is chiral symmetric, there are two robust

zero-energy in-gap states related by  $P$ . To satisfy the half-filling condition, one of the zero-energy states should be occupied while the other is unoccupied by introducing an infinitesimal perturbation breaking inversion. Then, a half-charge is accumulated at one corner while a half-charge is depleted at the other corner, when the charge is counted with respect to the half-filled configuration.

The location of anomalous corner states are fixed at  $M_y$  invariant corners. One way to see this is to use the topological classification proposed by Geier et al. [7]. When a 2D system has commuting mirror and chiral symmetries, it belongs to  $\text{BDI}^{M++}$  class that supports nontrivial topology, and the corresponding insulator has zero modes at mirror invariant corners. In MGD, the  $M_y$  symmetry commutes with chiral symmetry since  $M_y$  symmetry does not mix different sublattices. On the other hand, when chiral symmetry and  $M_x$  symmetry anti-commute, the system belongs to  $\text{BDI}^{M+-}$  class, which is topologically trivial, so there is no protected corner charges.

To be specific, we can find the location of corner states by studying the low-energy Hamiltonian of MGD near the  $\Gamma$  point:

$$H(k_x, k_y) = \hbar v(k_x \Gamma_1 + k_y \Gamma_2) + \Delta \Gamma_3, \quad (6)$$

where  $\Gamma_1 = \sigma_x \tau_x$ ,  $\Gamma_2 = \sigma_y \tau_x$ ,  $\Gamma_3 = \tau_z$ , and  $\Gamma_4 = \sigma_z \tau_x$ . Corresponding symmetry representations are  $T = \sigma_x \tau_z K$ ,  $P = \tau_z$ ,  $M_x = \sigma_x \tau_z$ ,  $M_y = \sigma_x$ , and chiral symmetry  $S$  is described by  $S = \Gamma_5 = \tau_y$ . Considering a disk-shaped geometry, the low-energy Hamiltonian in real space becomes  $H = -i\Gamma_1(\theta)\partial_r - i\Gamma_2(\theta)r^{-1}\partial_\theta + \Delta(r)\Gamma_3$ , where  $\Gamma_1(\theta) = \cos\theta\Gamma_1 + \sin\theta\Gamma_2$  and  $\Gamma_2(\theta) = -\sin\theta\Gamma_1 + \cos\theta\Gamma_2$ . We assume that  $\Delta(r) > 0$  inside the bulk and  $\Delta(r) < 0$  outside the bulk. The edge Hamiltonian is obtained by applying the projection operator  $P(\theta) = \frac{1}{2}(1 + i\Gamma_1(\theta)\Gamma_3)$ , leading to  $H_{\text{edge}} = -iR^{-1}\tilde{\sigma}_z\partial_\theta$  where  $\tilde{\sigma}_z = P\Gamma_2(\theta)P^{-1}$ . On the edge, position-dependent mass terms that open the edge gap are allowed. Mass terms that are commuting with  $P(\theta)$  and anti-commuting with  $\Gamma_2(\theta)$  and  $S$  are  $H_m = m_4(R, \theta)\Gamma_4 + im_{25}(R, \theta)\tilde{\Gamma}_2\Gamma_5$ . The corresponding edge Hamiltonian is  $H_{\text{edge}} = -iR^{-1}\tilde{\sigma}_z\partial_\theta + \tilde{m}_1(R, \theta)\tilde{\sigma}_x$ , where  $\tilde{m}_1 = m_4 + m_{25}$ ,  $\tilde{\sigma}_x = P\Gamma_4P^{-1} = Pi\tilde{\Gamma}_2\Gamma_5P^{-1}$ . Here  $PT$  symmetry requires  $\tilde{m}_1(\theta + \pi) = -\tilde{m}_1(\theta)$  while  $M_y$  requires  $\tilde{m}_1(x, y) = -\tilde{m}_1(x, -y)$ . Thus, the mass gap is closed at  $M_y$  invariant corners leading to localized corner charges.

In reality, however, chiral symmetry is broken so that the in-gap states are shifted from zero energy and can be merged into bulk states. Nevertheless, MGD still possesses corner charges. To prove this, let us illustrate how the number of states can be counted in a finite-size higher-order topological insulator with  $w_2 = 1$  following Ref. [10]. When the total number of states is  $N$  and chiral symmetry exists, there are  $N/2 - 1$  occupied and unoccupied states, respectively, since two in-gap states appear at zero energy. When chiral symmetry is broken while inversion is preserved, the two in-gap states related by inversion are absorbed into either the valence or the conduction bands simultaneously. Then the number of states below

the gap is  $n_{\text{gap}} = N/2 \pm 1$ . Therefore  $n_{\text{gap}} = [\frac{N}{2} + \text{an odd integer}]$  when  $w_2 = 1$ , whereas  $n_{\text{gap}} = [\frac{N}{2} + \text{an even integer}]$  when  $w_2 = 0$ . Since an odd number of electrons are filled below the gap in the higher-order topological insulator, a half electric charge should be accumulated (or depleted) at two corners.

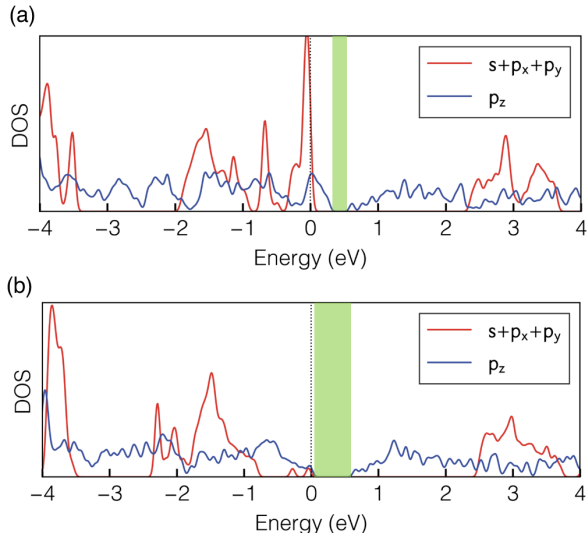


FIG. 3: (Color online) (a) Density of states (DOS) of a finite-size MGD without hydrogen passivation. Here the carbon atom at each corner has a non-bonding state. There are  $(4n - 1)$  holes below the gap at half-filling. The green color indicate the gapped region. (b) DOS of a finite-size MGD with hydrogen passivation where  $(8n - 4)$  hydrogen atoms are attached along the boundary. Here only two carbon atoms at  $M_y$  invariant corners have non-bonding states. There is a single hole below the gap at half-filling. Since both systems in (a) and (b) have an odd number of holes, both are higher-order topological insulators with  $w_2 = 1$ .

For the finite-size MGD composed of  $n \times n$  unit cells, the total number of states are  $N = 72n^2$  when  $2s$ ,  $2p_x$ ,  $2p_y$ , and  $2p_z$  orbitals are considered. According to the tight-binding model with chiral symmetry, there is a single  $sp$  electron localized at every edge of the hexagonal unit cell. When an edge of a unit cell is not shared with an adjacent unit cell, the relevant  $sp$  orbital becomes a half-filled zero-energy non-bonding state. Considering the geometry of a finite-size structure shown in Fig. 2, MGD has  $8n - 2$  non-bonding states along the boundary. When chiral symmetry is broken,  $8n - 2$  states can be merged into the valence band, so that  $n_{\text{gap}} = 36n^2 + 4n - 1 = \frac{N}{2} + 4n - 1$ . This is what is observed in first-principles calculations and the corresponding density of states is shown in Fig. 3 (a). Thus, when all the states below the gap are occupied, a half-integral charge (modulo an integer charge) is accumulated at the  $M_y$  invariant corners. This can be easily understood since there are an odd number of non-bonding states only at the  $M_y$  invariant corners.

To see the corner states more clearly, we add a hydrogen atom to the carbon atom at every corner, except at the two  $M_y$  invariant corners, and keep  $PT$  and  $M_y$  symmetries. Then

the number of added hydrogen atoms is an integer multiple of four, which does not alter the band topology of MGD. When two hydrogen atoms are added at the  $M_y$  invariant corners, the total number of bands becomes  $N' = N + 2$ , while  $n_{\text{gap}}$  remains the same as described in Fig. 4. Then  $n_{\text{gap}} = \frac{N'}{2} + 4n - 2$  and  $w_2$  becomes trivial. Therefore, the number of added hydrogen atoms should be an integer multiple of four to keep  $w_2$  unchanged. Maximally,  $(8n - 4)$  hydrogen atoms can be added to the finite-size MGD with two non-bonding states remaining at  $M_y$  invariant corners. The corresponding density of states is shown in Fig. 3 (b). Here half electric charges are accumulated at the  $M_y$  invariant corners of MGD when the states below the gap are occupied.

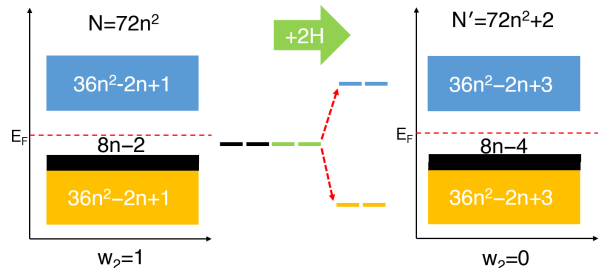


FIG. 4: (Color online) A schematic figure displaying the energy spectrum of a finite-size system where a thick black strip near the Fermi level indicates the non-bonding states arising from carbon atoms along the boundary. When two hydrogen atoms are added to the finite-size MGD with  $n \times n$  unit cells, the total number of states increases by two and the number of bands below the gap changes from  $\frac{N}{2} + 4n - 1$  to  $\frac{N'}{2} + 4n - 2$ . Then,  $w_2$  also changes from 1 to 0. Thus, to maintain the value of  $w_2$ , the number of hydrogen atoms attached for passivation should be an integer multiple of four.

*Discussion.*— Since MGD has  $w_2 = 1$ , when layers of MGD are stacked vertically, the resulting 3D insulator that preserves  $PT$  symmetry becomes a 3D weak Stiefel-Whitney insulator when inter-layer coupling is weak [16]. When inter-layer coupling becomes large, an accidental band crossing can happen at a TRIM at which a pair of nodal lines with  $Z_2$  monopole charge can be created. Such a 3D nodal line semimetal with two nodal lines at  $k_z = \pm k_c$  ( $k_c > 0$ ) was predicted in ABC-stacked graphdiyne [17] and the  $Z_2$  monopole charge of the nodal lines was also confirmed [16] based on first-principles calculations. In ABC-stacked graphdiyne, the 2D subspace with a fixed  $k_z$  carries  $w_2 = 1$  ( $w_2 = 0$ ) when  $|k_z| < k_c$  ( $k_c < |k_z| < \pi$ ) since the band inversion is happened at  $\mathbf{k} = (0, 0, \pi)$ . Since a 2D higher-order topological insulator with  $w_2 = 1$  possesses corner charges, similar corner charges are also expected in ABC-stacked graphdiyne in the subspace with a fixed  $k_z$  where  $w_2 = 1$ , which leads to hinge modes of the 3D structure shown in Fig 5 (a).

To confirm the presence of hinge modes of ABC-stacked graphdiyne, we study a tight-binding model by using only  $p_z$  orbitals to reduce numerical costs. The energy spectrum of a finite-size system with  $PT$  and  $M_x$  symmetries is shown in

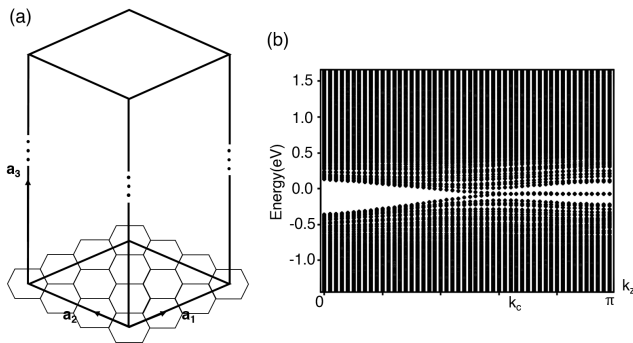


FIG. 5: (Color online) (a) A schematic figure describing the 3D geometry of ABC-stacked graphdiyne which is finite in the  $xy$  plane but periodic in the vertical direction. The structure must preserve  $C_{2x}$  symmetry to carry hinge states. (b) Hinge modes, located in the region  $k_c < |k_z| < \pi$ , obtained by tight-binding Hamiltonian using only  $p_z$  orbitals. In real materials including all core electronic levels, the hinge modes should appear in the region  $0 < |k_z| < k_c$  where  $w_2 = 1$ .

Fig 5 (b), which clearly shows the presence of hinge modes in the momentum region where  $w_2 = 1$  as expected. When only  $p_z$  orbitals are included, although the low-energy band structure from the tight-binding model is consistent with that from first-principles calculations, the topological property is different. Namely, the tight-binding model predicts  $w_2 = 0$  ( $w_2 = 1$ ) when  $|k_z| < k_c$  ( $k_c < |k_z| < \pi$ ), which is opposite to the result from the first-principles calculations. Such a discrepancy can be remedied when the core electronic levels are included in the tight-binding calculation, which is confirmed by separate calculations. To experimentally confirm the existence of corner charges in MGD and hinge modes in ABC-stacked graphdiyne is definitely an interesting problem for future studies.

We acknowledge the helpful discussions with Dongwook Kim and Youngkuk Kim. E. L., R. K. and J.A. were supported by IBS-R009-D1. B.-J.Y. was supported by the Institute for Basic Science in Korea (Grant No. IBS-R009-D1) and Basic Science Research Program through the National Research Foundation of Korea (NRF) (Grant No.0426-20180011), and the POSCO Science Fellowship of POSCO TJ Park Foundation (No.0426-20180002). This work was supported in part by the U.S. Army Research Office under Grant Number W911NF-18-1-0137..

*Note added.*— During the preparation of our manuscript, we have found a related work [30]. In [30], the authors also observed HOTI phase in MGD. However, some of the theoretical arguments are inconsistent with our results. For instance, in [30], it is stated that crystalline symmetries are not essential for the protection of corner states, which is in sharp contrast to our paper where the role of  $PT$  symmetry is emphasized. Also, in [30], it is mentioned that double band inversion of  $p_z$  orbitals at the  $\Gamma$  point is the origin of the HOTI phase. This is different from our result in that higher-order band topology

originates from the core levels derived from  $s, p_x, p_y$  orbitals.

\* equal contribution

† Electronic address: bjiang@snu.ac.kr

- [1] F. Schindler, A. M. Cook, M. G. Vergniory, Z. Wang, S. S. Parkin, B. A. Bernevig, and T. Neupert, *Science advances* **4**, eaat0346 (2018).
- [2] E. Khalaf, *Physical Review B* **97**, 205136 (2018).
- [3] J. Langbehn, Y. Peng, L. Trifunovic, F. von Oppen, and P. W. Brouwer, *Physical review letters* **119**, 246401 (2017).
- [4] F. Schindler, Z. Wang, M. G. Vergniory, A. M. Cook, A. Murani, S. Sengupta, A. Y. Kasumov, R. Deblock, S. Jeon, I. Drozdov, et al., *Nature physics* **14**, 918 (2018).
- [5] W. A. Benalcazar, B. A. Bernevig, and T. L. Hughes, *Science* **357**, 61 (2017).
- [6] See Supplemental Material.
- [7] M. Geier, L. Trifunovic, M. Hoskam, and P. W. Brouwer, *Physical Review B* **97**, 205135 (2018).
- [8] G. Van Miert and C. Ortix, *Physical Review B* **98**, 081110 (2018).
- [9] Z. Wang, B. J. Wieder, J. Li, B. Yan, and B. A. Bernevig, arXiv preprint arXiv:1806.11116 (2018).
- [10] B. J. Wieder and B. A. Bernevig, arXiv preprint arXiv:1810.02373 (2018).
- [11] J. Ahn and B.-J. Yang, arXiv preprint arXiv:1810.05363 (2018).
- [12] C. Yue, Y. Xu, Z. Song, H. Weng, Y.-M. Lu, C. Fang, and X. Dai, *Nature Physics* p. 1 (2019).
- [13] J. Ahn, S. Park, and B.-J. Yang, arXiv preprint arXiv:1808.05375 (2018).
- [14] E. Lee, A. Furusaki, and B.-J. Yang, arXiv preprint arXiv:1903.02737 (2019).
- [15] M. Ezawa, *Physical Review B* **98**, 045125 (2018).
- [16] J. Ahn, D. Kim, Y. Kim, and B.-J. Yang, *Physical review letters* **121**, 106403 (2018).
- [17] T. Nomura, T. Habe, R. Sakamoto, and M. Koshino, *Physical Review Materials* **2**, 054204 (2018).
- [18] J. Zak, *Physical review letters* **62**, 2747 (1989).
- [19] D. Xiao, M.-C. Chang, and Q. Niu, *Reviews of modern physics* **82**, 1959 (2010).
- [20] Z. Song, T. Zhang, and C. Fang, *Physical Review X* **8**, 031069 (2018).
- [21] L. Fu and C. L. Kane, *Physical Review B* **76**, 045302 (2007).
- [22] Y. Kim, B. J. Wieder, C. Kane, and A. M. Rappe, *Physical review letters* **115**, 036806 (2015).
- [23] T. L. Hughes, E. Prodan, and B. A. Bernevig, *Physical Review B* **83**, 245132 (2011).
- [24] A. M. Turner, Y. Zhang, R. S. Mong, and A. Vishwanath, *Physical Review B* **85**, 165120 (2012).
- [25] H. C. Po, A. Vishwanath, and H. Watanabe, *Nature Communications* **8**, 50 (2017).
- [26] Y. Zhao and Y. Lu, *Physical review letters* **118**, 056401 (2017).
- [27] C. Fang, Y. Chen, H.-Y. Kee, and L. Fu, *Physical Review B* **92**, 081201 (2015).
- [28] R. Yu, X. L. Qi, A. Bernevig, Z. Fang, and X. Dai, *Physical Review B* **84**, 075119 (2011).
- [29] A. Alexandradinata, X. Dai, and B. A. Bernevig, *Physical Review B* **89**, 155114 (2014).
- [30] X. Sheng, C. Chen, H. Liu, Z. Chen, Y.X. Zhao, Z. Yu, and S.A. Yang, arXiv preprint arXiv:1904.09985 (2019).